

## Metal-nonmetal transition in tungsten bronzes: A photoemission study

G. Hollinger and P. Pertosa

*Institut de Physique Nucléaire (et IN2P3) Université Claude Bernard (Lyon I),  
43 boulevard du 11 Novembre 1918, F-69622 Villeurbanne Cédex, France*

J. P. Doumerc

*Laboratoire de Chimie du Solide du CNRS, Université de Bordeaux I, 351 Cours de la Libération, F-33405 Talence, France*

F. J. Himpsel and B. Reihl\*

*IBM T. J. Watson Research Center, Yorktown Heights, New York 10598*

(Received 12 February 1985)

$\text{Na}_x\text{WO}_3$  and  $\text{Na}_x\text{Ta}_y\text{W}_{1-y}\text{O}_3$  bronzes are studied near the metal-nonmetal transition (MN) using core-level and valence-band photoelectron spectroscopy with synchrotron radiation. It is shown that in the semiconducting composition an impurity band with a width constant with  $x-y$  develops in the matrix  $p-d$  gap and that the density of states at the Fermi level is finite for compositions on both sides of the MN transition. These results show that the MN transition is due to localization in an impurity band in a pseudogap. This impurity band merges with the matrix conduction band when  $x-y$  increases.

### I. INTRODUCTION

The sodium tungsten bronzes  $\text{Na}_x\text{WO}_3$  present a metal-nonmetal transition (MN) when the sodium concentration approaches  $x \sim 0.25$ .<sup>1,2</sup> The transport properties of these compounds have been widely discussed the past ten years but no real consensus has been found on the origin of the MN transition.<sup>3-7</sup>

In these nonstoichiometric compounds the sodium atoms are inserted into interstitial sites of the  $\text{WO}_3$  lattice and  $x$  can vary between 0 and 1. A series of crystal structures exist depending on the concentration of the sodium atoms.<sup>2</sup> The cubic perovskite-type phase is stable for  $x > 0.4$ . The electronic structure of the metallic cubic,  $\text{Na}_x\text{WO}_3$  bronzes has been extensively studied from the experimental<sup>3,8-10</sup> and theoretical<sup>11-13</sup> point of view and the band structure is now well understood. The valence band which is formed predominantly from oxygen  $2p$  orbitals is separated from the conduction band by a gap of about 2 eV. The conduction band derives from the  $\pi$  antibonding overlapping of  $5d$  ( $t_{2g}$ ) tungsten orbitals and  $2p$  oxygen orbitals; no significant contribution of the sodium  $3s$  and  $3p$  orbitals has been found. In  $\text{WO}_3$  the conduction band is empty, leading to an insulating behavior. In  $\text{Na}_x\text{WO}_3$  the sodium atoms are ionized and give their  $3s$  electron to the conduction band of the  $\text{WO}_3$  matrix. The conduction band is therefore partially filled and a metallic behavior is expected. The validity of this elementary band picture was confirmed by a recent photoemission study<sup>10</sup> covering the high concentration range  $0.4 \leq x \leq 0.85$ . It was shown that the  $x$ -dependent variation of the shape of the occupied conduction band can be simply understood in terms of filling of a rigid  $\text{WO}_3$  conduction band. However, the conventional band theory fails to describe the semiconducting properties for low sodium concentrations.

A percolation approach was first considered to take ac-

count of the MN transition in the bronzes. Webman, Jortner, and Cohen<sup>5</sup> have given a treatment based on the assumption of metallic  $\text{NaWO}_3$  clusters of 45 Å extent in  $\text{WO}_3$ . This model was later strongly criticized by several authors.<sup>6,14-16</sup> Using Fuch's ideas,<sup>17</sup> Lightsey<sup>3</sup> performed a percolation analysis of the  $x$  dependence of the conductivity and Hall coefficient in a composition range down to  $x = 0.22$ . In the model proposed by Lightsey the linkage between each unit cell containing a Na atom can occur by first-, second-, and third-nearest neighbors. More recently Mott<sup>6</sup> has reexamined the problem and has compared the tungsten bronzes to heavily doped semiconductors, particularly the Si:P system. Such systems can be viewed in terms of a lattice of impurity states embedded in a host matrix. The electrons are assumed to occupy hydrogenic impurity states. Mott<sup>18</sup> derived a simple expression relating the first Bohr radius of an isolated center to the critical density of centers at the MN transition. Edwards and Sienko<sup>19</sup> showed that this law can be applied to a large number of semiconductors including the  $\text{WO}_3:\text{Na}$  tungsten bronzes. Focusing on the origin of the MN transition in the bronzes, Mott<sup>6</sup> discussed three possibilities: (i) the random charge distribution due to the  $\text{Na}^+$  cations leads to strong scattering and Anderson localization in the conduction band, (ii) an impurity band is formed and localization due to lateral disorder sets in for  $x \sim 0.2$ , (iii) an impurity band is split, resulting from electron correlations and Anderson localization occurs first in a pseudogap. Mott proposed that (i) was the correct description, whereas (ii) or (iii) occurs for Si:P. Each possibility evoked by Mott is associated to a specific band diagram. These diagrams are hypothetical and have been just compared indirectly to macroscopic measurements such as electrical resistivity, Hall coefficient, specific heat, magnetic susceptibility, etc. It was obvious that being able to investigate experimentally these band diagrams would be

of great interest for getting some understanding of the nature of the MN transition.

Photoelectron spectroscopy is a probe of the electronic density of states and should provide information on these problems. In previous x-ray photoemission spectroscopy (XPS) measurements<sup>20</sup> the relatively low energy resolution in conduction-band spectra coupled with the uncertainty in the Fermi-level position and problems resulting from the surface preparation of the samples<sup>21</sup> has prevented anyone from drawing a definitive conclusion on the  $x$ -dependent properties of the electronic structure. However, in an investigation on metallic cubic bronzes we have recently shown<sup>10</sup> that high-energy-resolution photoelectron spectroscopy coupled with a good surface preparation (cleavage of single crystals) can provide a very precise picture of the density of occupied states in the conduction-band region.

In this paper we present a study of the conduction-band region for semiconducting and metallic tungsten bronzes using photoelectron spectroscopy with synchrotron radiation. Because the MN transition cannot be observed directly in the  $\text{Na}_x\text{WO}_3$  system we also studied Ta-substituted tungsten bronzes of formula  $\text{Na}_x\text{Ta}_y\text{W}_{1-y}\text{O}_3$  which keep their cubic symmetry on both sides of MN transition.<sup>22</sup> Tantalum has one  $d$  electron less than tungsten and consequently  $x-y$  electrons populate the conduction band.

## II. EXPERIMENTAL PROCEDURES

Angle-integrated photoelectron spectra were measured with a two-dimensional display-type spectrometer combined with a toroidal grating monochromator in the (20–120)-eV photon range at the Synchrotron Radiation Center of the University of Wisconsin-Madison. Valence-band spectra were measured at 60 eV with an overall resolution better than 250 meV. W 4*f* and Ta 4*f* core levels were measured at 110 eV with a lower resolution (400 meV). The cubic  $\text{Na}_x\text{WO}_3$  and  $\text{Na}_x\text{Ta}_y\text{W}_{1-y}\text{O}_3$  crystals were cleaved along a (100) plane at a pressure of  $2 \times 10^{-10}$  Torr and studied at  $5 \times 10^{-11}$  Torr. The semiconducting  $\text{Na}_{0.1}\text{WO}_3$  samples having a tetragonal  $\text{WO}_3$ -related structure have been fractured in the same vacuum conditions. Thanks to the highly focused synchrotron radiation it was possible to investigate semiconducting  $\text{Na}_x\text{Ta}_y\text{W}_{1-y}\text{O}_3$  crystals with dimensions as small as 1 mm  $\times$  0.5 mm  $\times$  0.5 mm without interference with the sample holder. That is impossible with conventional XPS equipment.

## III. RESULTS AND DISCUSSION

Figures 1–4 give the core-level spectra in the W 4*f* region and valence-band spectra for series of  $\text{Na}_x\text{WO}_3$  and  $\text{Na}_x\text{Ta}_y\text{W}_{1-y}\text{O}_3$  bronzes. The core level spectra show the same trends as in the usual XPS spectra<sup>9,23</sup> except for the much higher cross section of the Na 2*p* level with the present photon energy (110 eV) and the presence of a sodium Na 2*p* surface sensitive component. These spectra are representative of the bulk properties of the bronzes. However some structures in the  $p$ - $d$  gap may arise from surface defects.

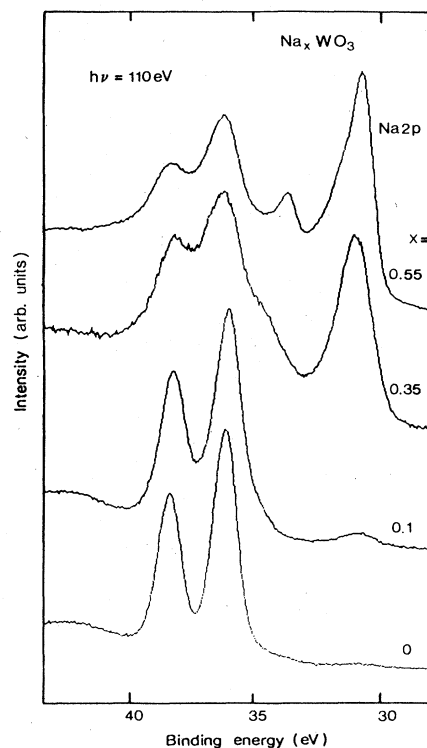


FIG. 1. Photoemission spectra at  $h\nu=110$  eV of the W 4*f* region for  $\text{Na}_x\text{WO}_3$  as a function of  $x$ .

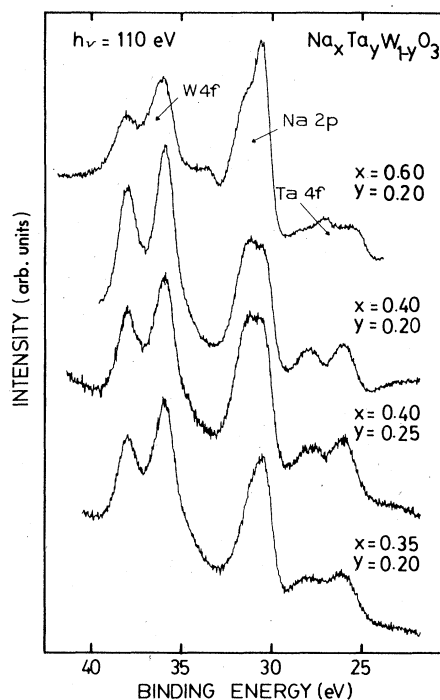


FIG. 2. Photoemission spectra at  $h\nu=110$  eV of the W 4*f* and Ta 4*f* region for  $\text{Na}_x\text{Ta}_y\text{W}_{1-y}\text{O}_3$  as a function of  $x$  and  $y$ .

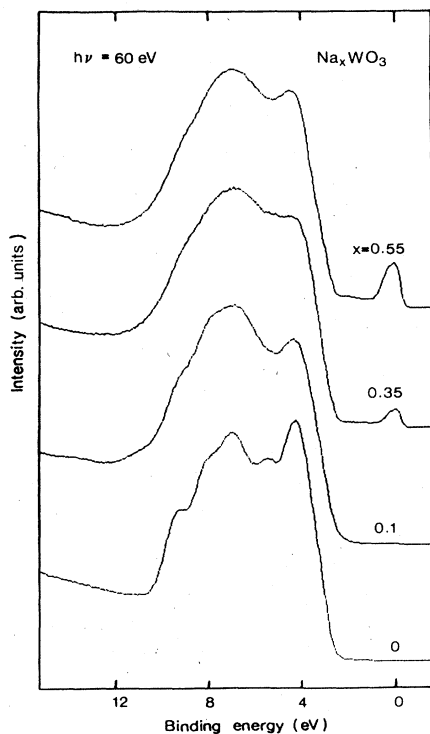


FIG. 3. Photoemission spectra at  $h\nu=60$  eV of the valence-band region for  $\text{Na}_x\text{WO}_3$  as a function of  $x$ .

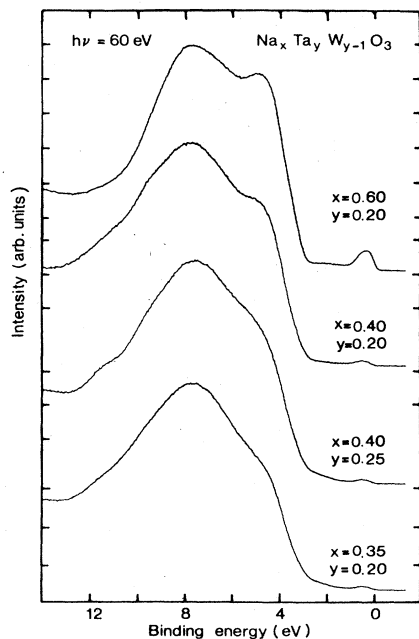


FIG. 4. Photoemission spectra at  $h\nu=60$  eV of the valence-band region for  $\text{Na}_x\text{Ta}_y\text{W}_{1-y}\text{O}_3$  as a function of  $x$  and  $y$ .

The W  $4f$  and Ta  $4f$  core-level spectra of  $\text{Na}_x\text{WO}_3$  and  $\text{Na}_x\text{Ta}_y\text{W}_{1-y}\text{O}_3$  are characterized by at least two overlapping  $4f_{5/2}$ ,  $4f_{7/2}$  doublets whereas  $\text{WO}_3$  shows only one doublet. The origin of these doublets in metallic bronzes has been widely discussed,<sup>8,24</sup> but no simple explanation exists yet. We decided not to use these data in the discussion of the present results. On the other hand, there is no difficulty in interpreting the shape of the core-level spectra in the semiconducting range: The two doublets are simply related to the existence of  $\text{W}^{6+}$  and  $\text{W}^{5+}$  tungsten states.  $\text{W}^{6+}$  states are present before the photoemission process and  $\text{W}^{5+}$  states correspond to electrons delocalized in the impurity band (as will be discussed below) on tungsten atoms affected by Na ions and then localized on a particular W atom as the result of core ionization. The intensity of these  $\text{W}^{5+}$  components can be directly correlated to the number of occupied states in the conduction band region. A first important result is therefore that electrons which give  $\text{W}^{5+}$  features in the  $4f$  spectra and in the conduction band region are localized on tungsten sites. In  $\text{Na}_x\text{Ta}_y\text{W}_{1-y}\text{O}_3$ ,  $4f$  doublets are observed for both W and Ta components. This means that  $d^0$  and  $d^1$  configurations exist for both W and Ta atoms.

In Figs. 5 and 6 we have expanded the conduction band region of the  $\text{Na}_x\text{WO}_3$  and  $\text{Na}_x\text{Ta}_y\text{W}_{1-y}\text{O}_3$  spectra, respectively. In Figs. 5(a) and 6(a) the spectra are shifted with the high-energy sides matched together in order to test an eventual rigid-band behavior. In this model the width of the occupied part of the conduction band is expected to increase with  $x$  or  $x-y$ . It is seen clearly that

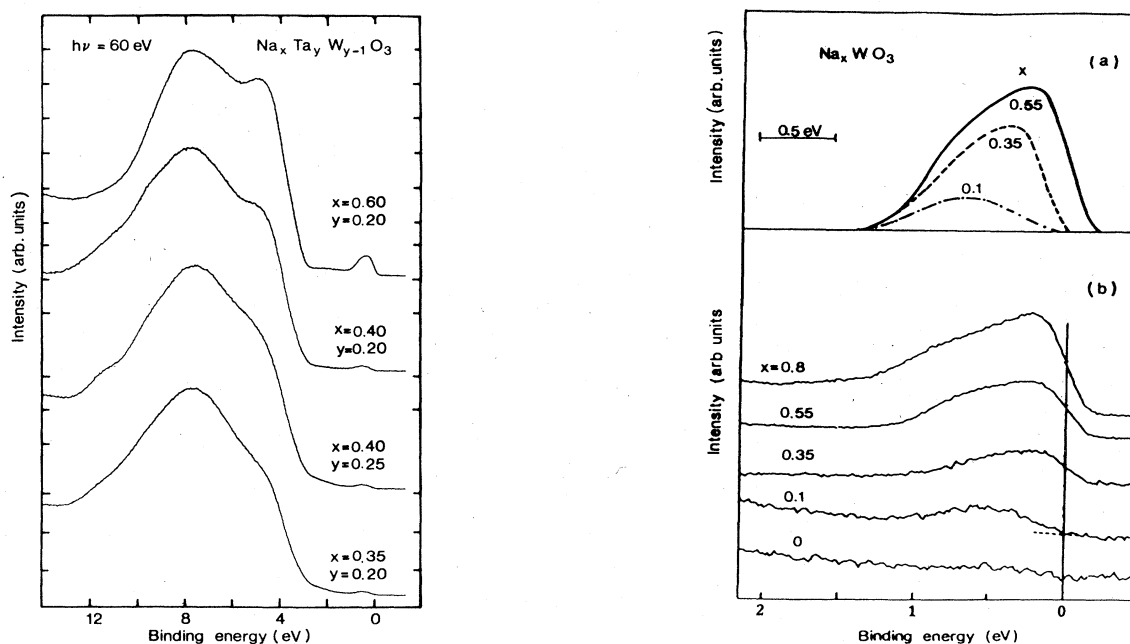


FIG. 5. Conduction band spectra measured at 60 eV versus  $x$  for  $\text{Na}_x\text{WO}_3$ . In (a) after background subtraction the high-energy sides are matched together in order to test a rigid band behavior; in (b) the raw spectra are presented with the Fermi levels aligned.

nonrigid band behavior exists when semiconducting compounds are compared to metallic compounds. In the semiconducting range the width of the conduction band remains constant (it is about 1.1 eV wide) when  $x$  or  $x-y$  vary. A second point is that the shape of the band is nearly symmetrical and does not seem to correspond to filling of a band.

Figures 5(b) and 6(b) give the conduction-band spectra with the Fermi levels aligned. It was possible to define very accurately the position of the Fermi level. The uncertainty was only  $\pm 0.05$  eV. For metallic bronzes we observe the usual Fermi cutoff convoluted by the experimental broadening function. For a very low conduction-electron concentration ( $\text{Na}_{0.1}\text{WO}_3$  or  $\text{Na}_{0.25}\text{Ta}_{0.20}\text{W}_{0.8}\text{O}_3$ ) no detectable density of states exists at the Fermi energy. However when  $x-y$  approaches the value for which the MN transition occurs ( $x-y \approx 0.3$ ) (Refs. 25 and 26) a finite density of states is observed at the Fermi level [ $x-y=0.15$  and  $0.20$  in Fig. 6(b)].

A final piece of information is given by the values of the  $p-d$  gap between valence and conduction states. We estimate the values of the gap at  $1.8 \pm 0.15$  eV and  $1.7 \pm 0.15$  eV, respectively, for  $\text{Na}_x\text{WO}_3$  and  $\text{Na}_x\text{Ta}_y\text{W}_{1-y}\text{O}_3$ .

The present data cannot be simply explained by the filling of the  $\text{WO}_3$  conduction band. On the contrary, they seem to characterize an impurity band in the  $\text{WO}_3$  gap as far as sodium atoms are inserted. From our photoemission results it is possible to determine the  $p-d$  energy difference between the valence band and the conduction

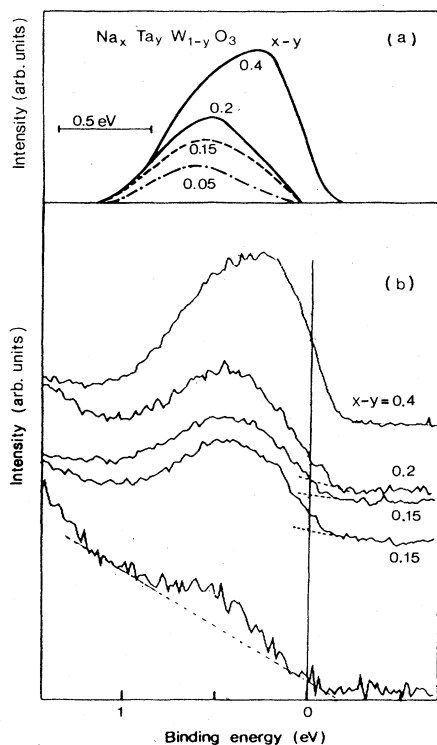


FIG. 6. Same as Fig. 5 for  $\text{Na}_x\text{Ta}_y\text{W}_{1-y}\text{O}_3$ .

states and to evaluate the shape and the width of the occupied part of the impurity band. However, we cannot evaluate exactly the value of the  $p-d$  gap between the matrix valence band and the matrix conduction band for the semiconducting bronzes. For monoclinic  $\text{WO}_3$  a 2.77 eV-wide gap was found experimentally,<sup>27</sup> which would locate the impurity band just below the matrix conduction band.

In Fig. 7 we have schematized the densities of states corresponding to three concentration regimes: (a) the semiconducting range with very low conduction electron concentration, (b) the semiconducting range near the MN transition, and (c) the metallic range.

As already pointed out, the impurity band arising in the upper side of the matrix gap seems to be filled up for very low  $x$  or  $x-y$  values. The levels of this impurity band are provided by  $5d t_{2g}$  orbitals of tungsten (or tantalum) atoms situated in the immediate vicinity of one or several  $\text{Na}^+$  ions. For regular uncompensated semiconductors the Fermi level is expected to be in the middle of the impurity band whereas with a compensation less than half of the band (for  $n$ -type behavior) should be occupied.<sup>28</sup> The fact that for already small  $x$  (or  $x-y$ ) values the band seems completely filled could result from a splitting into two Hubbard bands due to correlation effects as usually in doped semiconductors.<sup>28</sup>

As  $x$  (or  $x-y$ ) increases, the energy difference between impurity band states, and matrix conduction band states decreases, which can lead to overlapping of both bands: a finite density of states is expected at the Fermi level [Fig. 7(b)] and observed for  $x-y=0.20$  and  $0.15$  [Fig. 6(b)]. However the samples with  $x-y=0.20$  and  $0.15$  have a thermally activated electrical conductivity.<sup>25,26</sup> Such a behavior can only be explained by an electronic localization in states situated at the Fermi level. Such an Anderson-type localization can be due to a disorder resulting from a random distribution of  $\text{Na}^+$  and  $\text{Ta}^{5+}$  ions.

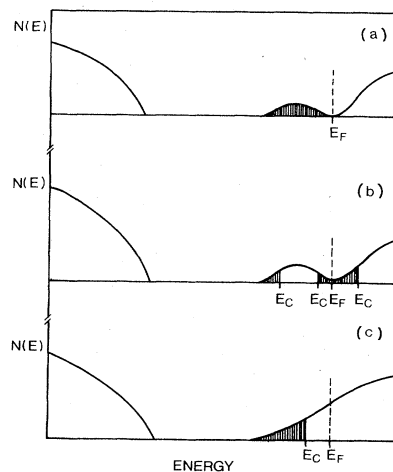


FIG. 7. Schematic band diagram for semiconducting [(a) and (b)] and metallic (c) sodium tungsten bronzes. Anderson localized states are shaded.

When the sodium insertion rate is large, i.e., about 50%, all transition-element sites become nearly equivalent and the impurity band merges into the conduction band of the bronze, but a tail of localized states may subsist [Fig. 7(c)].

It seems that the Fermi level is within a pseudogap rather than just below the top of the impurity band as Fig. 6(b) could also suggest for  $x - y = 0.20$  and  $0.15$ . In the latter case a positive thermoelectric power would be expected. On the contrary a negative value has been experimentally observed<sup>26</sup> (its absolute value increase with temperature,<sup>26</sup> which means that the predominant carriers are electrons at the Fermi level rather than electrons excited above the mobility edge into the conduction band).

It appears thus that the MN transition in the tungsten bronzes is mainly due to Anderson localization in a pseudogap. This situation is close to the (iii) scheme proposed by Mott and described above, with a pseudogap between the lower Hubbard band and the conduction band rather than between the two Hubbard bands.

Our conclusions are actually not very far from prediction of Edgell *et al.*<sup>29</sup> These authors have examined by ultraviolet photoemission spectroscopy (UPS) the conduction band of polycrystalline  $\text{Na}_x\text{WO}_3$  samples. They suggested the existence of an impurity band splitted by electronic correlations. In fact these kind of models are exactly those used for describing the MN transition in doped semiconductors. The difference between Si- and

$\text{WO}_3$ -based systems is that the associated hydrogenic Bohr radius is large in silicon ( $\approx 30$  Å) and very short in  $\text{WO}_3$  ( $\approx 3$  Å). Therefore, the transition appears in silicon at a much lower donor concentration than in  $\text{WO}_3$ . The hydrogenoid approximation is very rough for  $\text{WO}_3$  because real impurity states are made of W  $5d$  orbitals which are known to be much more localized than  $s$  or  $p$  orbitals. Finally we may notice that, if we keep the hydrogenoid approximation, it is not surprising that a percolation treatment which assumes about the same radius for metallic units gives correct values for the donor concentration at the MN transition.

#### IV. CONCLUSION

By measuring directly the density of states in semiconducting and metallic tungsten bronzes, it was possible to show that the metal-nonmetal transition is due to localization in a pseudogap between a sodium-induced  $5d t_{2g}$  metallic band and the conduction band of the matrix.

#### ACKNOWLEDGMENTS

We gratefully acknowledge the assistance of the staff of the Synchrotron Radiation Center of the University of Wisconsin-Madison. We would also like to thank Professor P. Hagenmuller for a critical reading of the manuscript.

\*Present address: IBM Zurich Research Laboratory, CH-8803 Rüchlikon, Switzerland.

<sup>1</sup>B. W. Brown and E. Banks, *J. Am. Chem. Soc.* **76**, 963 (1954).

<sup>2</sup>P. Hagenmuller, *Prog. Solid State Chem.* **5**, 71 (1971).

<sup>3</sup>P. A. Lightsey, *Phys. Rev. B* **8**, 3586 (1973).

<sup>4</sup>P. A. Lightsey, D. A. Lilienfeld, and D. F. Holcomb, *Phys. Rev. B* **14**, 4730 (1976).

<sup>5</sup>C. Webman, J. Jortner, and M. H. Cohen, *Phys. Rev. B* **13**, 713 (1976).

<sup>6</sup>N. F. Mott, *Philos. Mag.* **35**, 111 (1977).

<sup>7</sup>B. R. Weinberger, *Phys. Rev. B* **17**, 566 (1978).

<sup>8</sup>M. Campagna, G. K. Wertheim, H. R. Shanks, F. Zumsteg, and E. Banks, *Phys. Rev. Lett.* **36**, 1393 (1976).

<sup>9</sup>J. N. Chazalviel, M. Campagna, G. K. Wertheim, and H. R. Shanks, *Phys. Rev. B* **16**, 697 (1977).

<sup>10</sup>G. Hollinger, F. J. Himpsel, B. Reihl, P. Pertosa, and J. P. Doumerc, *Solid State Commun.* **44**, 1221 (1982).

<sup>11</sup>J. B. Goodenough, *Prog. Solid State Chem.* **5**, 145 (1971).

<sup>12</sup>L. Kopp, B. N. Harmon, and S. H. Lin, *Solid State Commun.* **22**, 677 (1977).

<sup>13</sup>D. W. Bullett, *J. Phys. C* **16**, 2197 (1983); *Solid State Commun.* **46**, 575 (1983).

<sup>14</sup>D. P. Tunstall, *Phys. Rev. B* **14**, 4735 (1976).

<sup>15</sup>R. S. Crandall and B. W. Faughnan, *Phys. Rev. B* **16**, 1750 (1977).

<sup>16</sup>G. Hollinger and P. Pertosa, *Chem. Phys. Lett.* **74**, 341 (1980).

<sup>17</sup>R. Fuchs, *J. Chem. Phys.* **42**, 3781 (1965).

<sup>18</sup>N. F. Mott, *Can J. Phys.* **34**, 1356 (1956).

<sup>19</sup>P. P. Edwards and M. J. Sienko, *Phys. Rev. B* **17**, 2575 (1978).

<sup>20</sup>H. Hochst, R. D. Bringans, and H. R. Shanks, *Phys. Rev. B* **26**, 1702 (1982).

<sup>21</sup>Since the photoemission technique probes a very shallow region near the surface it is very important that the surface composition reflects the bulk composition. We think that the best way to prepare surfaces for bronzes is to cleave single crystals under vacuum. We know from previous experiments that using filing techniques as did authors of Ref. 20 may induce surface oxygen losses.

<sup>22</sup>J. P. Doumerc, J. Marcus, M. Pouchard, and P. Hagenmuller, *Mater. Res. Bull.* **14**, 201 (1979).

<sup>23</sup>G. Hollinger *et al.* (unpublished).

<sup>24</sup>G. Hollinger, F. J. Himpsel, N. Martensson, B. Reihl, J. P. Doumerc, and T. Akahane, *Phys. Rev. B* **27**, 6370 (1983).

<sup>25</sup>J. P. Doumerc, P. Dordor, E. Marquestaut, M. Pouchard, and P. Hagenmuller, *Philos. Mag. B* **42**, 487 (1980).

<sup>26</sup>P. Dordor, J. P. Doumerc, and G. Villeneuve, *Philos. Mag. B* **47**, 315 (1983).

<sup>27</sup>G. Hoppmann and E. Salje, *Opt. Commun.* **30**, 199 (1979).

<sup>28</sup>N. F. Mott and E. A. Davis, *Electronic Processes in Non-Crystalline Materials*, 2nd ed. (Clarendon, Oxford, 1979).

<sup>29</sup>R. G. Edgell and M. D. Hill, *Chem. Phys. Lett.* **85**, 140 (1982); *J. Phys. C* **16**, 6205 (1983).